molecular pharmaceutics

ACS AuthorChoice

Article

pubs.acs.org/molecularpharmaceutics

Terms of Use

Crystal Engineering of Green Tea Epigallocatechin-3-gallate (EGCg) Cocrystals and Pharmacokinetic Modulation in Rats

Adam J. Smith,[†] Padmini Kavuru,[§,⊥] Kapildev K. Arora,[§,∥] Sheshanka Kesani,[§] Jun Tan,[‡] Michael J. Zaworotko,*[,§] and R. Douglas Shytle*[,†,‡]

[†]Center of Excellence for Aging and Brain Repair, Department of Neurosurgery and Brain Repair, USF Health College of Medicine, University of South Florida, Tampa, Florida 33612, United States

[‡]Neuroimmunology Laboratory, Silver Child Development Center, Department of Psychiatry and Neurosciences, USF Health College of Medicine, University of South Florida, Tampa, Florida 33620, United States

[§]Department of Chemistry, College of Arts and Sciences, University of South Florida, Tampa, Florida 33620, United States

[∥]Pfizer Global Research & Development, Groton, Connecticut 06340, United States

Supporting Information

ABSTRACT: The most abundant polyphenol in green tea, epigallocatechin-3-gallate (EGCg), has recently received considerable attention due to the discovery of numerous health-promoting bioactivities. Despite reports of its poor oral bioavailability, EGCg has been included in many dietary supplement formulations. Conventional preformulation methods have been employed to improve the bioavailability of EGCg. However, these methods have limitations that hinder the development of EGCg as an effective therapeutic agent. In this study, we have utilized the basic concepts of crystal engineering and several crystallization techniques to screen for various solid crystalline forms of EGCg and evaluated the efficacy of crystal engineering for modulating the pharmacokinetics of EGCg. We synthesized and characterized seven previously undescribed crystal forms of EGCg including the pure crystal structure of EGCg. The aqueous solubility profiles of four new EGCg cocrystals were determined. These cocrystals were subsequently dosed at 100 mg EGCg per kg body weight in rats, and the plasma levels were monitored over the course of eight hours following the single oral dose. Two of the EGCg cocrystals were found to exhibit modest improvements in relative bioavailability. Further, cocrystallization resulted in marked effects on pharmacokinetic parameters including C_{max}, T_{max}, area under curve, relative bioavailability, and apparent terminal half-life. Our findings suggest that modulation of the pharmacokinetic profile of EGCg is possible using cocrystallization and that it offers certain opportunities that could be useful during its development as a therapeutic agent.

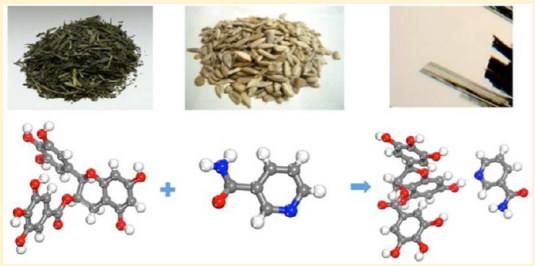

KEYWORDS: *green tea, EGCg, cocrystal, bioavailability, solubility, pharmacokinetics, Alzheimer's disease, vitamin B3, crystal engineering, dissolution rate*

INTRODUCTION

Bioflavonoids are a group of polyphenolic compounds that are common throughout the plant kingdom. They are widely studied and have been found to promote healthy living in epidemiologic studies.[1,2] Much of the attention that bioflavonoids have attracted is due mainly to the "*French paradox*". This is the dietary anomaly in which people in the Mediterranean culture have a higher fat intake but a lower incidence of cardiovascular disease and increased longevity.[3] This phenomenon has been largely attributed to increased dietary intake in bioflavonoids.

One of the most widely studied bioflavonoids is, epigallocatechin-3-gallate (EGCg), the most abundant polyphenol in green tea. It has been studied extensively during the past decade for its therapeutic potential in various cancers,[4−8] Alzheimer's disease,[9−12] obesity,[13,14] and diabetes.[15,16] Despite these promising therapeutic uses, the plasma concentrations of EGCg that are required are prohibitively high. Thus, novel methods for improving the oral bioavailability of EGCg are desirable. In a previous study, we demonstrated that proprietary nanolipidic particles could be used to improve the bioactivity of EGCg for reducing amyloid beta production in a cell model of Alzheimer's disease while also more than doubling the oral bioavailability.[17] Although this could potentially overcome the problems thwarting the clinical translation of EGCg, the technology is limited because it requires an alcohol suspension.

Until now there have been no reports of any of the crystalline forms of EGCg in the Cambridge Structural Database (CSD) including the crystal structure of pure EGCg which makes it worth studying from a structural perspective. Therefore, we undertook the synthesis of cocrystals of EGCg and also

Received: February 12, 2013
Revised: May 17, 2013
Accepted: June 3, 2013
Published: June 3, 2013

crystallized its pure form. This was accomplished by taking advantage of crystal engineering concepts and several crystallization techniques. Cocrystallization, crystals formed from two or more components or "cocrystal formers (CCFs)", has emerged over the past decade as a materials science approach to generate novel solid forms of active pharmaceutical ingredients with improved physicochemical properties.[18−29] We recently reported four new cocrystal forms of another flavonoid, quercetin, which improved solubility by up to *14-fold* and oral bioavailability by up to *10-fold*.[27] Unlike quercetin, EGCg is highly soluble in water.[30] Previous pharmacokinetics experiments have shown that EGCg is absorbed rapidly in the gut following oral administration.[31,32] However, membrane permeability of EGCg is reported to be low.[33,34] Thus, EGCg would likely fall into the Biopharmaceutics Classification System (BCS) 3: high solubility, low permeability. We hypothesized that new cocrystals of EGCg with reduced water solubility might exhibit pharmacokinetic profiles that are more desirable for drug development. Moreover, we hypothesized that reducing the solubility would decrease the rate of dissolution and slow the absorption of EGCg *in vivo*. We report herein the results of our structural, solubility, and pharmacokinetic studies.

EXPERIMENTAL SECTION

Reagents and Materials. Green tea-derived EGCg (>95% purity by HPLC) was purchased from http://www.herbs-tech.com. Isonicotinamide (INM, >99% purity), isonicotinic acid (INA, >99% purity), nicotinamide (NIC, >99% purity), and nicotinic acid (NAC, 98% pure) were purchased from Sigma-Aldrich Corporation (St. Louis, MO, USA).

Preparation of Single Crystals. All crystallization and cocrystallization experiments were either conducted at room temperature or at 4 °C. The solvents were distilled prior to their use. Specific experimental details are as follows.

Form II. EGCg (65.0 mg, 0.14 mmol) was dissolved in 1 mL of acetonitrile (99% pure). The resulting solution was layered on 2.5 mL of dichloromethane and was allowed to stand in the refrigerator. Colorless platelet crystals were harvested after three days.

Form III. EGCg (200.0 mg, 0.436 mmol) was dissolved in 2.5 mL of acetonitrile (99% pure). The solution was layered onto 6 mL of dichloromethane and 2 mL of nitrobenzene and then allowed to stand in a refrigerator. Yellow crystalline needles were harvested after 24 h.

Form IV. The pure crystal line form of EGCg, Form IV, was obtained by heating Forms II or III at 120° for 20−25 min. Form IV crystals can also be reproduced by dissolving EGCg (45.0 mg 0.098 mmol) in 1 mL of acetonitrile (99% pure). The solution was layered on 2.5 mL of dichloromethane and seeded with form IV and was allowed to stand in the refrigerator. After one week colorless needle-like crystals were observed.

EGCgINM·5H$_2$O. EGCg (45.80 mg, 0.099 mmol) and *iso*-nicotinamide (99% pure, used as received, 12.2 mg, 0.0998 mmol) were dissolved in 5 mL of water. Colorless block-like crystals of EGCgINM·5H$_2$O were harvested in less than 5 min. However to further grow better quality crystals, 1:1 water/methanol (v/v %) solvent was used, and the crystals were obtained in one day.

EGCgNIC·9H$_2$O. EGCg (45.80 mg, 0.099 mmol) and nicotinamide (99% pure, used as received, 12.2 mg, 0.0998 mmol) were dissolved in 2 mL of water. A cluster of crystals were obtained after three days. Looking carefully under the microscope a colorless block like single crystal was separated from the cluster and was used for single crystal X-ray diffraction analysis.

EGCgINA·3H$_2$O. EGCg (45.80 mg, 0.099 mmol) and *iso*-nicotinic acid (99% pure, used as received, 12.3 mg, 0.0998 mmol) were dissolved in 5 mL of water. Colorless needles of EGCgINA·3H$_2$O were harvested in one day.

EGCgINA. The anhydrous form of EGCgINA·3H$_2$O was obtained by dehydrating the cocrystal.

EGCgNAC·xH$_2$O. EGCg (458.0 mg, 0.99 mmol) and nicotinic acid (99% pure, used as received, 123.0 mg, 0.998 mmol) were slurried in 2 mL of water overnight in a vial. The vial was left in the hood undisturbed, and after two days a cluster of block shaped crystals was obtained.

Thermogravimetric Analysis (TGA). TGA was performed on a Perkin-Elmer STA 6000 simultaneous thermal analyzer. Open alumina crucibles were used for analysis from 30 to 300 °C at 5 °C/min heating rate under nitrogen purge.

Differential Scanning Calorimetry (DSC). Thermal analysis was carried out employing a TA Instruments DSC 2920 differential scanning calorimeter. Standard aluminum pans were used for the experiment for all the samples. Temperature calibrations were made using indium as a standard. An empty pan, sealed in the same way as the sample, was used as a reference pan. A typical sample (2−8 mg) was heated in a DSC from 30 to 300 °C at a 5 °C/min heating rate. The experimental data were analyzed using commercially available software (TA Universal Analysis 2000; TA Instruments).

Infrared Spectroscopy (FT-IR). All of the forms of EGCg were characterized by infrared spectroscopy using a Nicolet Avatar 320 FT-IR instrument. The amount of the sample used was around 2−3 mg. The spectra were measured over the range of 4000−400 cm^{-1}. Data were analyzed by using EZ Omnic software.

Powder X-ray Diffraction (PXRD). The bulk samples were analyzed by powder X-ray diffractometry. The samples were placed on the sample holder with the help of vacuum grease and exposed, at room temperature, to Cu Kα radiation (λ = 1.54056 Å; 40 kV × 30 mA, Bruker AXS D8 advance). For all the samples, the angular range was 3−0° 2θ, with a step size of 0.05° 2θ. Intensity counts were accumulated for 0.5 s at each step. Data analyses were performed using commercially available software (PowderX and Origin).

Single-Crystal X-ray Data Collection and Structure Determinations. Single crystals of Forms II, III, and IV and cocrystals EGCgINM·5H$_2$O, EGCgNIC·9H$_2$O, EGCgINA·3H$_2$O, and EGCgNAC·xH$_2$O were examined under a microscope, and suitable crystals were selected for single crystal X-ray crystallography. Single crystal X-ray diffraction data on Forms III and IV were collected on a Bruker-AXS SMART APEX CCD diffractometer with monochromatized Mo Kα radiation ((λ = 0.71073 Å), whereas for Form II and cocrystals EGCgINM·5H$_2$O, EGCgNIC·9H$_2$O, EGCgINA·3H$_2$O, and EGCgNAC·xH$_2$O, data were collected on a Bruker-AXS SMART APEX 2 CCD diffractometer with monochromatized Cu Kα radiation (λ = 1.54178 Å). Both of the diffractometers are connected to a KRYO-FLEX low temperature device. Indexing was performed using APEX2[35] (Difference Vectors method). Data integration and reduction were performed using SaintPlus 6.01.[36] Absorption correction was performed by a multiscan method implemented in SADABS.[37] Space groups were determined using XPREP implemented in APEX2.[35] The structure was solved using SHELXS-97 (direct methods) and

Table 1. Crystallographic Data and Structure Refinement Parameters

	Form II	Form III	Form IV	EGCgINM·5H_2O
formula	$C_{22.5}H_{20.5}N_{1.5}O_{12.3}Cl_{0.5}$	$C_{28}H_{25}NO_{14}$	$C_{22}H_{18}O_{11}$	$C_{28}H_{24}N_2O_{17}$
MW	561.04	599.49	458.36	660.49
crystal system	monoclinic	orthorhombic	monoclinic	monoclinic
space group	*C*2	$P2_12_12_1$	$P2_1$	*C*2
a (Å)	23.072 (5)	13.161 (3)	12.959 (12)	19.603 (8)
b (Å)	14.908 (4)	13.169 (3)	5.669 (5)	14.491 (6)
c (Å)	15.806 (4)	14.536 (4)	13.094 (12)	10.585 (4)
α (deg)	90	90	90	90
β (deg)	103.44 (2)	90	107.276 (13)	92.089 (7)
γ (deg)	90	90	90	90
V (Å^3)	5288.1 (2)	2519.4 (11)	918.6	3005 (2)
D_c (mg m^{-3})	1.409	1.581	1.657	1.460
Z	8	4	2	4
2θ range	2.87−67.72	2.09−25.35	1.65−25.35	1.75−25.02
N_{ref}/N_{para}	6591/830	4602/488	1854/370	4761/429
T (K)	100 (2)	100 (2)	100 (2)	298 (2)
R_1 [$I > 2\sigma(I)$]	0.0596	0.0356	0.0384	0.0671
wR_2	0.1624	0.0865	0.0872	0.1782
GOF	1.092	1.009	1.019	0.971
abs coef.	1.407	0.129	0.135	0.124

	EGCgNIC·9H_2O	EGCgINA·3H_2O	EGCgNAC·*x*H_2O
formula	$C_{28}H_{24}N_2O_{16.75}$	$C_{28}H_{29}NO_{16}$	$C_{28}H_{28}NO_{18}$
MW	656.49	547.88	666.51
crystal system	triclinic	orthorhombic	monoclinic
space group	*P*1	$P2_12_12_1$	*C*2
a (Å)	10.497 (2)	7.5068 (2)	19.9700 (4)
b (Å)	11.769 (2)	14.0136 (3)	14.1716 (3)
c (Å)	12.203 (2)	26.1150 (6)	10.5170 (2)
α (deg)	72.56 (3)	90	90
β (deg)	85.80 (3)	90	93.4720 (1)
γ (deg)	83.00 (3)	90	90
V (Å^3)	1426.4 (5)	2747.23 (11)	2970.9 (1)
D_c (g cm^{-3})	1.528	1.537	1.490
Z	2	4	4
2θ range	4.25−69.33	3.38−66.57	5.59−67.72
N_{ref}/N_{para}	7923/881	4747/426	4982/502
T (K)	173 (2)	100 (2)	100 (2)
R_1 [$I > 2\sigma(I)$]	0.0632	0.0598	0.0467
wR_2	0.1701	0.1542	0.1158
GOF	1.059	0.05642	1.038
abs coef.	1.118	1.062	1.101

refined using SHELXL-97 (full-matrix least-squares on F2) contained in APEX2[35] and WinGX v1.70.01[38−40] programs packages.

EGCgNAC·xH$_2$O. All non-hydrogen atoms were refined anisotropically. Hydrogen atoms of −CH and −CH2 groups were placed in geometrically calculated positions and included in the refinement process using a riding model with isotropic thermal parameters: U_{iso}(H) = 1.2U_{eq} (−CH2, −CH). Hydrogen atoms of −OH, −NH groups and water molecules have been found from difference Fourier map and refined using DFIX (d(O−H) = 0.84 Å for hydroxyl groups, DFIX −2.2 antibumping restraints for two H···H distances) and SADI restraints for water molecules (O−H and H···H distances) with U_{iso}(H) = 1.5U_{eq}(−OH). Some of water molecules were observed to be disordered in the structure. It was not possible to locate hydrogen atoms of those molecules.

EGCgNIC·9H$_2$O. All non-hydrogen atoms were refined anisotropically. Hydrogen atoms of −CH and −CH_2 groups were placed in geometrically calculated positions and included in the refinement process using riding model with isotropic thermal parameters: U_{iso}(H) = 1.2U_{eq}(−CH_2, −CH). Hydrogen atoms of −OH and −NH groups were placed in geometrically calculated position and refined using AFIX 147 and AFIX 93 correspondingly. Positions of hydrogen atoms H4, H15, and H25a were further refined using a distance restraint (H···O{H-bond acceptor}) of 1.865(8) Å as found from a CSD analysis. Some of the water molecules were observed to be disordered, and it was not possible to locate hydrogen atoms for those molecules.

EGCgINA·3H$_2$O. All non-hydrogen atoms were refined anisotropically. Hydrogen atoms of −CH and −CH_2 groups were placed in geometrically calculated positions and included in the refinement process using a riding model with isotropic thermal parameters: U_{iso}(H) = 1.2U_{eq}(−CH_2, −CH). Hydrogen atoms of −OH groups were placed in geometrically calculated position and refined using AFIX 147 or AFIX 83.

dx.doi.org/10.1021/mp4000794 | *Mol. Pharmaceutics* 2013, 10, 2948−2961

Water molecules were refined using distance restraints. The observed residual electron density 1.258 el/ Å^3 can probably be attributed to the presence of small satellite crystals and/or disordered chains of INA. Crystal data and refinement conditions are shown in Table 1.

Synthesis of Cocrystals in Bulk for Dissolution. The cocrystals EGCgINM·5H_2O, EGCgNIC·9H_2O, EGCgINA·3H_2O, and EGCgINA were made in bulk for dissolution studies using the slurry method. EGCgNAC·xH_2O was not included in the dissolution study due to difficulties in reproducing it in bulk powder form. Slurry experiments to reproduce EGCgNAC·xH_2O resulted in a glue-like material rather than a powder. For the remaining cocrystals, stoichiometric amounts of the starting materials were stirred overnight in 2−3 mL of water with the help of a magnetic stir bar on a stir plate that produced the cocrystals with 100% yield. The purity of the bulk material was tested by powder X-ray diffractometry (PXRD) and differential scanning calorimetry (DSC). A uniform particle size (between 53 and 75 μm) for the bulk powder was obtained for all the cocrystals and EGCg by sieving using standard ASTM sieves.

Cocrystal Solubility Evaluation. Solubility studies were performed on EGCg, EGCgINM·5H_2O, EGCgNIC·9H_2O, EGCgINA·3H_2O, and EGCgINA using UV/vis/NIR spectrophotometry in water at room temperature. The wavelength used for the determination of EGCg was 305 nm since there is no interference with the CCFs at this wavelength. The dissolution studies were conducted by taking approximately 3 g of the cocrystal in 50 mL of water and stirring with a magnetic stir bar at ca. 125 rpm for 4 h. Aliquots were drawn from the slurry at regular time intervals (5, 10, 15, 20, 25, 30, 45, 60, 75, 90, 120, 150, 180, and 240 min) and filtered using a 0.45 μm nylon filter. The filtrates were diluted appropriately and analyzed to measure the concentration of EGCg (at 305 nm) by using a UV/vis/NIR spectrometer. The remaining undissolved solid was analyzed by PXRD and DSC to confirm phase stability. The solubility measurements were done in replicates of three.

Pharmacokinetic Screening of EGCg Formulations in Rats. All animal studies were conducted in accordance with a University of South Florida IACUC-approved protocol. Male Sprague−Dawley rats (n = 3 per group) weighing 200−250 g were purchased from Harlan Laboratories (Indianapolis, IN). The rats were purchased precannulated by Harlan. The rounded tip catheters were surgically implanted into the jugular vein of the rats making multiple, precise blood draws painless to the animal. The rats were food (not water) deprived for 18 h prior to the start of the experiment. Corn oil was selected as the gavage vehicle because all crystal forms were observed to be insoluble in it. All EGCg forms were sieved to attain a particle size between 53 and 75 μm prior to suspending in corn oil at 20 mg of EGCg per mL. The EGCg formulations were delivered via oral gavage at a dosage of 100 mg EGCg per kg body weight. Blood was collected at the following time points: 0, 5, 10, 30, 60, 120, 240, and 480 min. Because heparin was kept in the catheter lines to prevent clotting, a small amount of blood was drawn and discarded before collecting each sample. Approximately 300 μL of blood was collected in EDTA tubes for each time point. The samples were kept on ice to preserve their integrity and then centrifuged at 4000 rpm for 10 min, after which the plasma was transferred to sterile centrifuge tubes. A preservative solution was added to each plasma sample at 10% (v/v) concentration to ensure the integrity of the EGCg during storage.[41] This preservative was comprised of 20% ascorbic acid (to prevent oxidation) and 0.1% EDTA (to scavenge any metal contaminants). The samples were stored at −80 °C until they were analyzed for EGCg content.

Quantification of EGCg in Rat Plasma. To accurately quantify the concentration of EGCg in the plasma, a previously described method was employed using liquid chromatography with tandem mass spectrometry.[42−44]

Stock Preparation. A 2.00 mg/mL stock solution of EGCg in DMSO was prepared. The standard spiking solutions were prepared by diluting the stock solution to 1000 and 100 μg/mL using acetonitrile−water (1:1, v:v). Both solutions were protected from light using amber vials, and all solutions were stored at −20 ∘C.

Standard Curve Preparation. For this analysis two standard curves were prepared: one with a higher (10−0.100 μg/mL) dynamic range, and the other a lower range (1000−10 ng/mL). Both standard curves were prepared using the appropriate blank plasma containing the preservative. The results indicated that the standard curve performance was within acceptable range for bioanalytical method acceptance (R^2 > 0.99).

Pharmacokinetic Calculations. Mean plasma EGCg concentrations and the standard error in the mean (SEM) were graphed using GraphPad PRISM software (GraphPad Software, Inc.). Phoenix WinNonlin Version 6.3 (Pharsight Corporation, Mountain View, CA) was used to conduct a noncompartmental analysis of the pharmacokinetic data and generate the pharmacokinetic parameters. The reported pharmacokinetic parameters included C_{max}, T_{max}, area under curve (AUC), relative bioavailability (F_{rel}), and apparent terminal half-life (HL_Lambda_z). Relative bioavailability was determined by dividing the mean AUC of each EGCg formulation by the control. All pharmacokinetic parameters are reported as mean and standard deviations.

Statistical Analysis. Two-tailed t-tests were used to assess the statistical significance at each time point for the pharmacokinetic curves. Each EGCg cocrystal was compared to the EGCg control at each time point. The criterion for rejection of the null hypothesis was P < 0.05.

RESULTS

Screening of EGCg Cocrystals and Its Pure Form. The CCFs were selected based on the supramolecular synthon

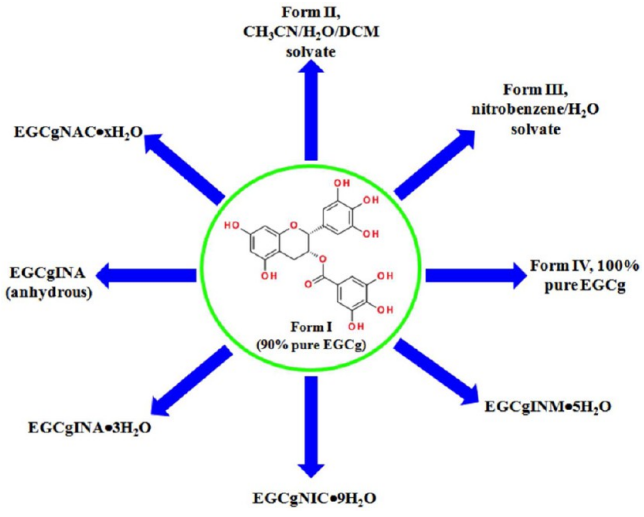

Figure 1. Graphical representation of the new EGCg crystal forms.

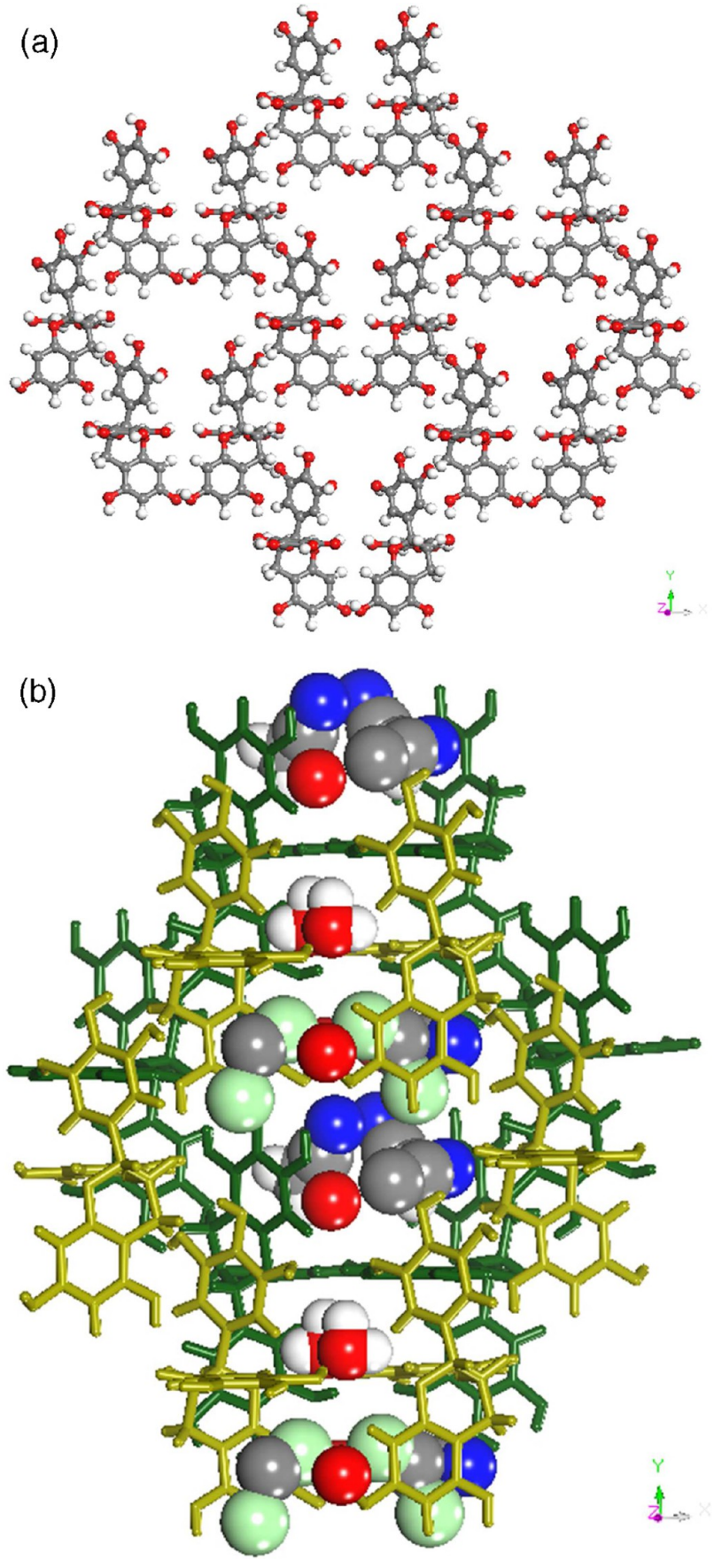

Figure 2. (a) EGCg molecules in Form II forming sheets with channels. (b) A typical channel being occupied by solvent molecules in Form II.

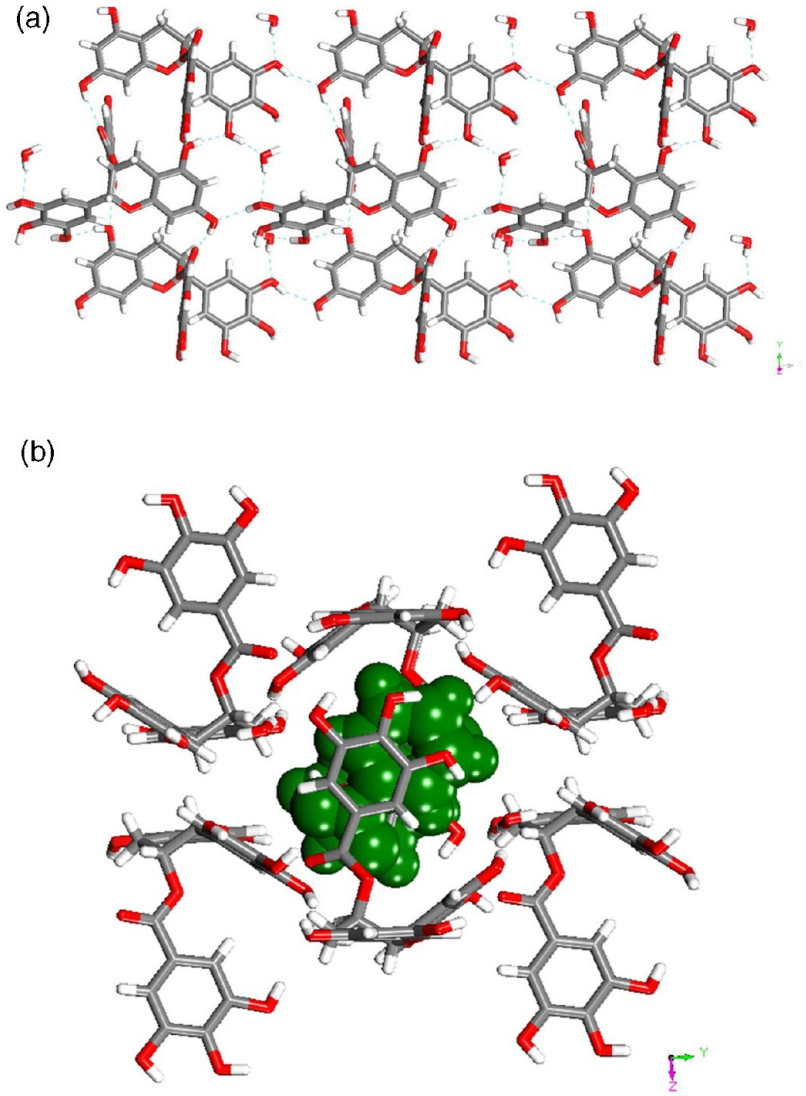

Figure 3. (a) Illustration of a representative sheet formed by EGCg and water molecules in Form III. (b) Nitrobenzene molecule sandwiched between sheets of EGCg and water molecules in Form III.

approach. According to this approach the CCFs were identified based on the functional groups present on EGCg and analyzing the frequency for the occurrence of supramolecular synthons (homo and hetero) with other functional moieties. This analysis was carried out via the CSD, an archive of over ~600 000 organic crystal structures. The CSD also offers a software platform that facilitates statistical analysis of packing motifs, thereby providing empirical information on common functional groups and how they associate at the molecular level. Several fragments of EGCg were identified, and a CSD analysis was conducted to determine if these fragments and/or the whole molecule (EGCg) are susceptible to form cocrystals with carboxylic acids, alcohols, or weak bases. Furthermore, the selected CCFs should be suitable for use in drug products (e.g., FDA approved, GRAS or EAFUS listed). Several potential CCFs were selected based on the above-mentioned criteria. However, we were unable to obtain cocrystals with any other CCFs except those presented herein. In addition, efforts to obtain pure crystalline forms of EGCg via different crystallization techniques led to the isolation of two solvates which upon desolvation resulted in a pure crystalline form of EGCg. Figure 1 illustrates the crystalline forms obtained during the screening process.

Interestingly, all of the isolated cocrystals are in the form of hydrates. EGCg is a large and flexible molecule containing a number of hydrogen bond donors and acceptors. This makes it prone to formation of hydrates. Furthermore, the raw material used is EGCg monohydrate, and dehydration of the starting material is reversible. Except for EGCgINA·$3H_2O$,all cocrystals became amorphous following dehydration. EGCgINA·$3H_2O$ upon dehydration yields an anhydrous cocrystal of EGCg and INA. We believe that water plays a pivotal role in crystallizing these cocrystals, but it is difficult to say whether the water molecules are playing a space-filling role in channels or they are an integral part of the crystal lattice.

Crystal Structure Descriptions. *Form II* *($2C_{22}H_{18}O_{11}·3CH_6CN·3H_2O·CH_2Cl_2$).* Form II crystallizes in the monoclinic *C*2 space group and is a high *Z*' structure consisting of two EGCg, three acetonitrile, three water, and a disordered dichloromethane molecule in the asymmetric unit. The two symmetry-independent EGCg molecules form sheets with voids that accommodate the solvent molecules, as shown in Figure 2a and b.

dx.doi.org/10.1021/mp4000794 | *Mol. Pharmaceutics* 2013, 10, 2948−2961

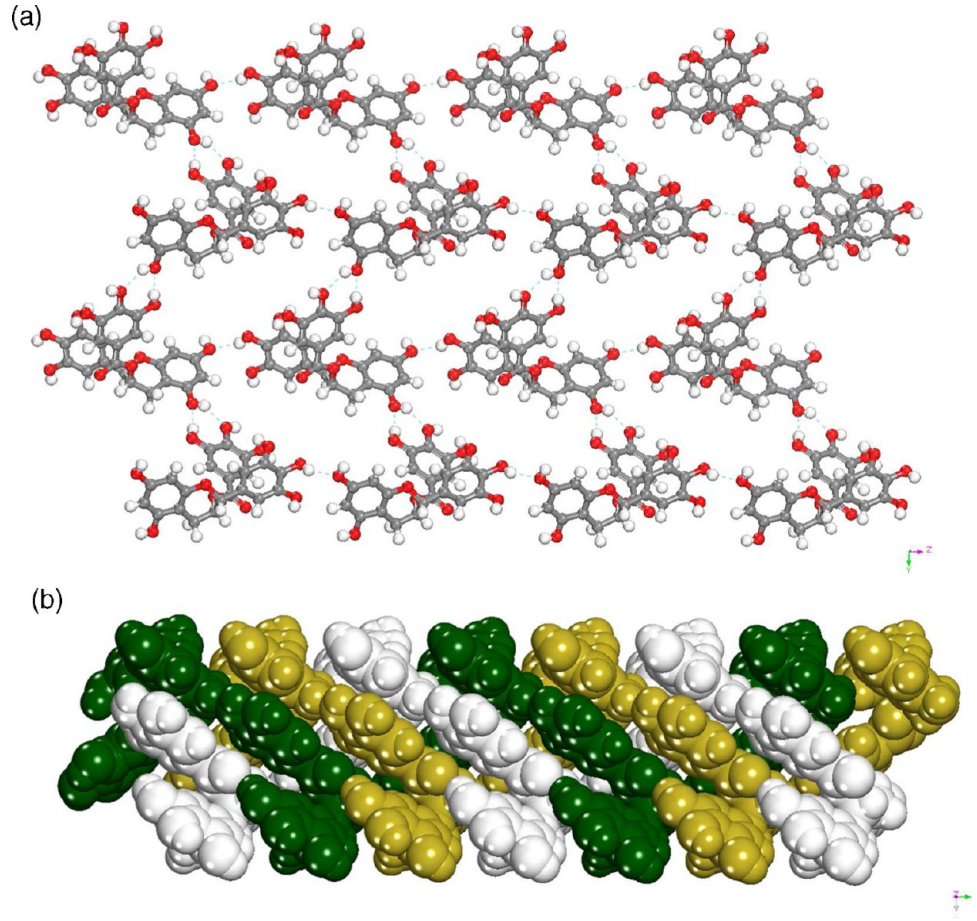

Figure 4. (a) Crystal packing of Form IV; crinkled sheets with cavities were created via several O−H···O H-bonds. (b) Self-interpenetrated 3D structure of Form IV.

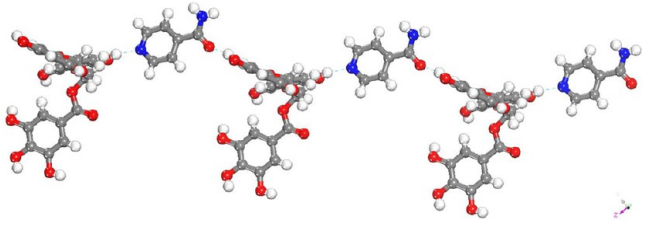

Figure 5. Intermolecular H-bonding between EGCg and INM molecules. Water molecules are removed for clarity.

Form III ($C_{22}H_{18}O_{11}·C_6H_5NO_2·H_2O$). Form III, a solvated form of EGCg with nitrobenzene and water, crystallized in the orthorhombic $P2_1$ space group with one molecule of each component in the asymmetric unit. In the crystal structure the EGCg and water molecules form sheets. One of the sheets is shown in Figure 3a.

Form IV. Pure EGCg, Form IV, crystallizes in monoclinic $P2_1$ space group with one EGCg molecule in asymmetric unit. The EGCg molecules form crinkled sheets with voids. The voids are interpenetrated with other sheets to exhibit 2-fold interpenetration as shown in Figure 4a and b.

EGCgINM·5H$_2$O. The single crystal X-ray structure analysis reveals that EGCgINM·5H_2O is a pentahydrate of the 1:1 cocrystal of EGCg and INM. EGCg molecules and INM molecules interact through one point hydrogen bonds (O−H···N, O···N: 2.756 (2) Å) between a hydroxyl group of EGCg molecules and the aromatic nitrogen of INM molecules. These dimeric units are further connected by O−H···O (O···O: 2.662 (4) Å) hydrogen bonds formed between hydroxyl moieties of EGCg and carbonyl moieties of INM molecules and thereby form zigzag chains as illustrated in Figure 5.

EGCgNIC·9H$_2$O. The crystallization of EGCg and NIC in water results in the formation of a 1:1 cocrystal nonahydrate. It crystallizes in $P1$ space group with two molecules each of EGCg and NIC molecules and nine water molecules in the asymmetric unit (Figure 6a). The N−H functionality of the NIC molecules interact with one of the O−H moieties present of ring A of EGCg with an N···O bond distance of 2.570 (2) Å (Figure 6b).

EGCgINA·3H$_2$O. The cocrystallization of EGCg and INA resulted in the formation of a cocrystal trihydrate which crystallizes in the orthorhombic space group $P2_1P2_1P2_1$. The INA and EGCg molecules interact with each other through water molecules (Figure 7a). One of the three water molecules interacts with two EGCg and one INA molecule through the following H-bonds: (a) the O−H of the water molecule interacts with the C−O moiety of the INA molecule with a bond distance of 2.739 (3) Å; (b) the O−H of the water molecule interacts with two neighboring EGCg molecules with H-bond distances of 2.704 (5) and 2.752 Å (3) Å. The other water molecule forms a trifurcated bond with three different EGCg molecules as presented in Figure 7b through O−H···O bonds of 2.667 (3), 2690 (2), and 2.712 (2) Å. The INA molecules form head to tail chains through N−H···O bifurcated hydrogen bonds (2.540 (2) and 2.986 (3) Å) (Figure 7a).

dx.doi.org/10.1021/mp4000794 | *Mol. Pharmaceutics* 2013, 10, 2948−2961

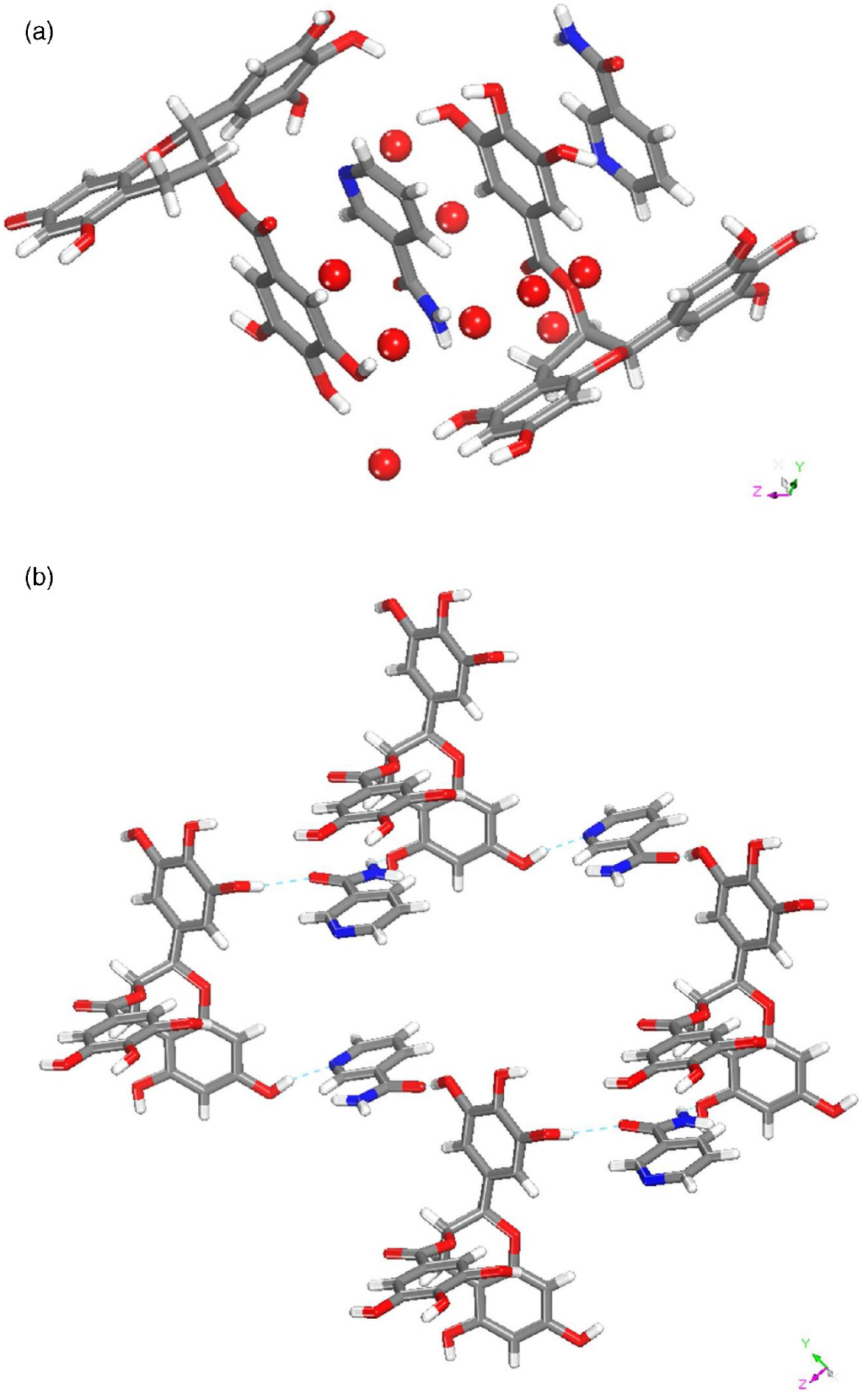

Figure 6. (a) Asymmetric unit of EGCgNIC·9H_2O cocrystal. (b) H-bonding between EGCg and NIC molecules.

EGCgNAC·xH_2O. The 1:1 cocrystal of EGCg and NAC crystallized as a hydrate in monoclinic space group *C*2. Unlike the other cocrystals the stiochiometry of water in the EGCg-nicotinic acid (NAC) is indefinite. We were unable to determine the number of water molecules in the crystal lattice of EGCg-NAC cocrystals due to poor quality crystals and single crystal data (see Table 1). From the crystal structure it is evident that NAC molecules exist as zwitterions unlike INA in

dx.doi.org/10.1021/mp4000794 | *Mol. Pharmaceutics* 2013, 10, 2948−2961

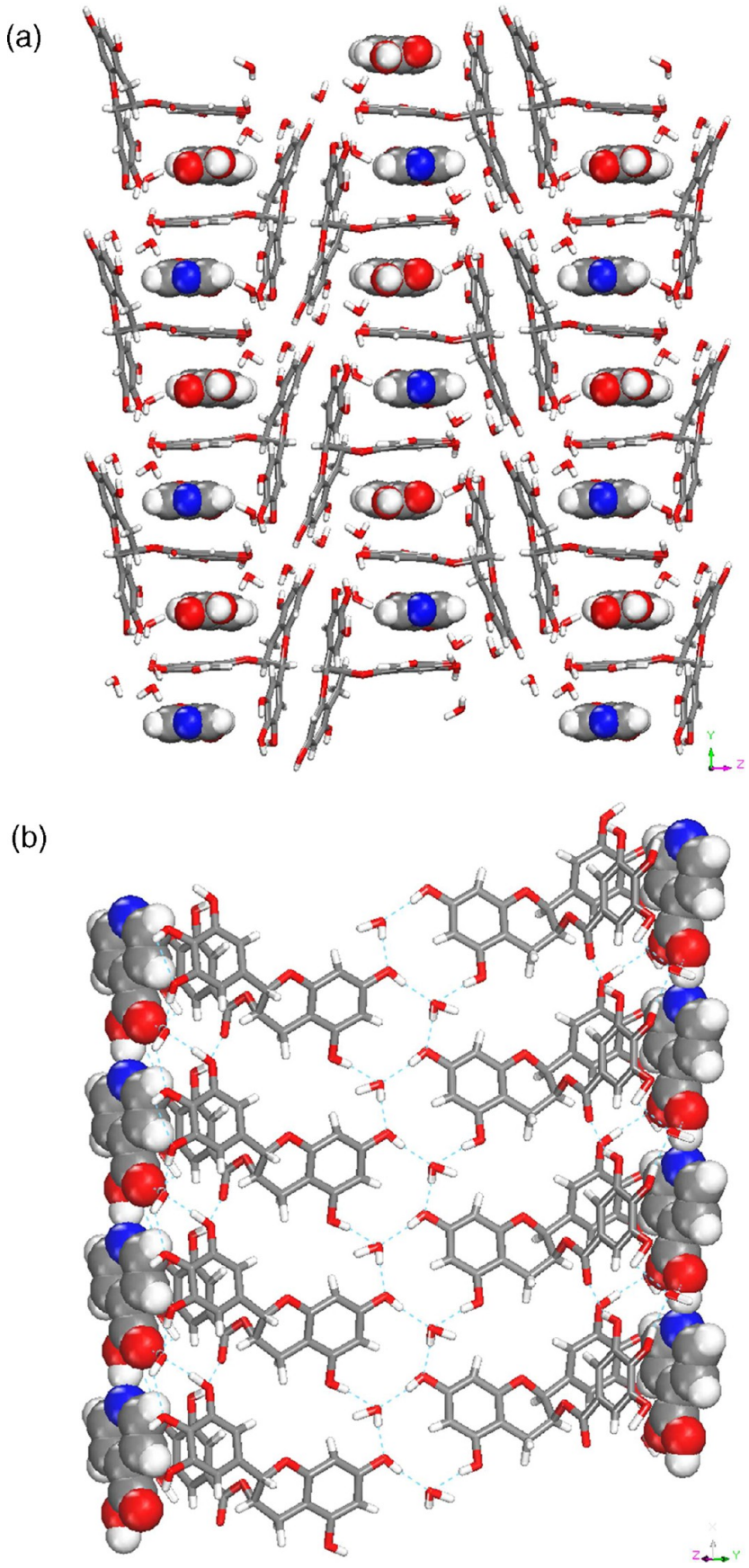

Figure 7. Crystal packing in EGCg·INA·3H_2O.

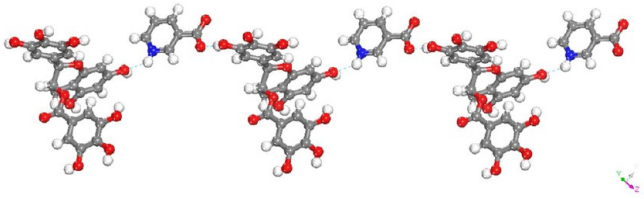

Figure 8. Illustration hydrogen bonding between EGCg and NAC molecules in EGCgNAC·xH$_2$O cocrystal (water molecules are not shown in the figure for clarity).

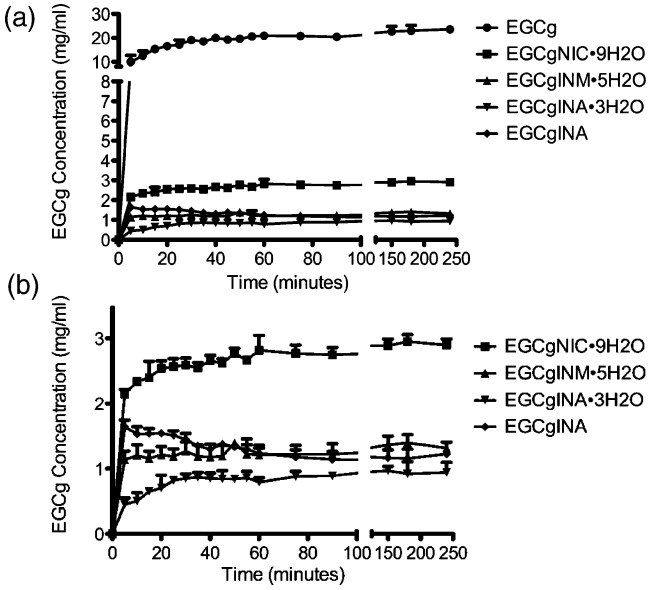

Figure 9. Dissolution profiles of (a) EGCg and its cocrystals and (b) the cocrystals alone in water.

Table 2. Aqueous Solubilities of EGCg and Its Cocrystals

compound	aqueous solubility after 4 h (mg/mL)
EGCg	23.60
EGCgINM·5H$_2$O	1.32
EGCgNIC·9H$_2$O	2.90
EGCgINA·3H$_2$O	0.94
EGCgINA	1.23
EGCgNAC·xH$_2$O	NA

EGCgINA·3H$_2$O. The C−N−C bond angle is 122.76°, and the C−O bond distances are 1.237 and 1.252 Å. One of the water molecules is disordered. Each of the NAC zwitterions interacts two neighboring EGCg molecules via the following H-bonds: (a) an H-bond formed between one of the O−H groups on ring B with one of the carboxylates of the NAC molecules at a distance of 2.588 (3) Å; (b) an H-bond between the N−H of the NAC molecule and one of the O−H functionalities present on ring A of another EGCg molecule (N−H···O: 2.902 (3) Å). The intermolecular H-bonding between EGCg and NAC zwitterions is illustrated in Figure 8.

Aqueous Solubility of EGCg Cocrystals. EGCg is relatively soluble in water compared to many other flavonoids such as quercetin. We determined the solubility profiles of the four new EGCg cocrystals reported herein and observed that all of the cocrystals exhibit reduced solubility. The solubility studies were conducted for 4 h because after 1 h it was observed that the solubilities remained almost constant and did not change for the next 3 h. This suggests that the solubilities had reached equilibrium after 1 h. Figure 9 shows the dissolution profiles of EGCg and the EGCg cocrystals. The maximum solubility of EGCg determined experimentally was approximately 23.6 mg/mL during the 4 h dissolution experiment. The EGCg cocrystals were found to exhibit far lower aqueous solubilities when compared to EGCg as illustrated in Figure 9. The cocrystal that exhibited the highest aqueous solubility was EGCgNIC·9H$_2$O (2.95 ± 0.11 mg/mL). EGCgINA (anhydrous), EGCgINM·5H$_2$O, and EGCgINA·3-H$_2$O were observed to exhibit solubilities of 1.227 ± 0.036, 1.401 ± 0.122, and 0.97 ± 0.07 mg/mL, respectively. The solubilities of EGCg and its cocrystals are tabulated in Table 2. After the dissolution experiment has concluded (4 h), the identity of the powders was confirmed by PXRD and DSC. EGCgINA anhydrous had converted to the hydrate form, EGCgINA·3H$_2$O, while the remaining cocrystals were found to be stable up to at least 4 h..

Pharmacokinetics of EGCg Cocrystals. The pharmacokinetic curves for EGCg and the EGCg cocrystals are presented in Figure 10. Each cocrystal is shown separately (solid line) against the EGCg control (dashed line). The EGCg cocrystals exhibited very different pharmacokinetic profiles. The pharmacokinetic parameters are shown in Table 3. EGCg peaked rapidly at 7.50 ± 2.74 min (T_{max}) due to its high solubility and consequent high rate of dissolution. The cocrystals peaked in the plasma in the following order: EGCgNIC·9H$_2$O, EGCgINM·5H$_2$O and EGCgINA·3H$_2$O, EGCgINA. Surprisingly, only two of the cocrystal forms resulted in improved bioavailability: EGCgINA·3H$_2$O and EGCgINA. These cocrystals had modest improvements in relative bioavailability at F_{rel} of 1.37 and 1.05, respectively. EGCg peaked more rapidly than all of the cocrystal forms and exhibited the shortest apparent terminal half-life, 249.35 ± 60.73 min. Interestingly, cocrystallization changed the overall shape of the pharmacokinetic curve. This was most apparent with the EGCgINA·3H$_2$O and EGCgINA cocrystals, which exhibited drastic changes in the time to reach maximal plasma concentrations (T_{max}) at 30.00 ± 24.49 and 160 ± 61.97 min, respectively. In some cases, these pharmacokinetic profiles might be advantageous to the rapid peak and elimination profile of free EGCg.

■ DISCUSSION AND CONCLUSIONS

EGCg research increased drastically when researchers reported that epidemiological evidence indicated lower rates of certain cancers in populations that consumed the most green tea. Since then, numerous molecular mechanisms for these beneficial properties have been discovered. Not surprisingly, EGCg has become one of the most popular nutraceutical ingredients in the world. However, reports of its poor bioavailability are troublesome to product development.[17,45−47] EGCg is highly susceptible to oxidation, first pass metabolism, and rapid efflux.[46] Numerous groups have evaluated delivery systems to overcome these limitations with EGCg, but none have tried cocrystallization. Cocrystallization has been used extensively to improve the solubility and/or bioavailability of poorly soluble APIs.[22,23,27,48−54] This study is the first report on the bioavailability effects of reducing the solubility of a highly soluble API.

We evaluated the structure, solubility, and pharmacokinetics of four new cocrystals of EGCg, all of which were found to exhibit reduced water solubility. We hypothesized that these changes in solubility would change the pharmacokinetics of

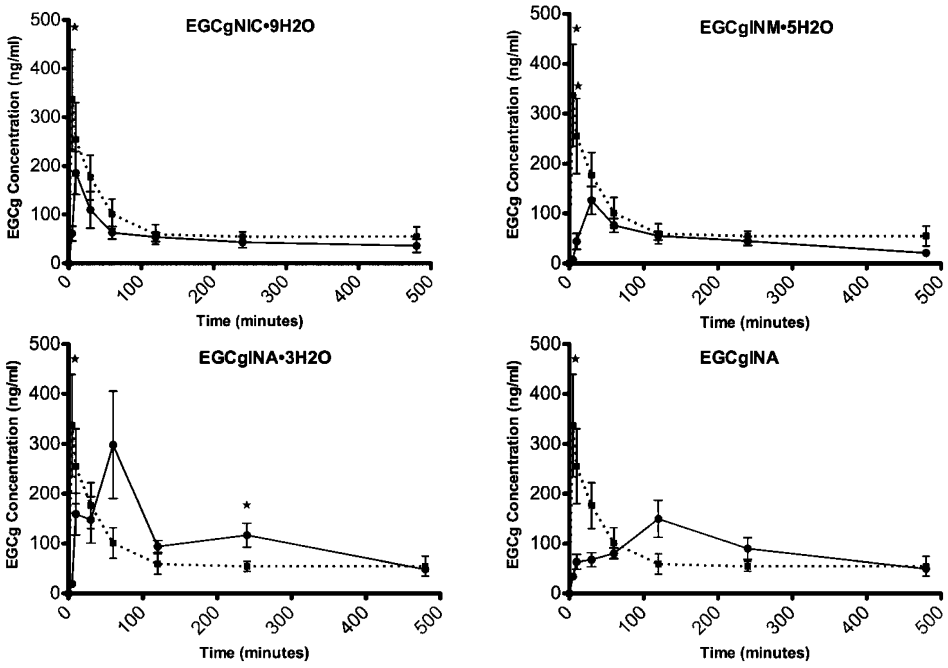

Figure 10. Pharmacokinetic profiles (mean plasma concentration + SEM versus time). The solid line in each panel represents the indicated EGCg cocrystal. The dashed lines are the EGCg control. There were three rats per group (n = 3). ★$P < 0.05$.

Table 3. Pharmacokinetic Parameters

	EGCg		EGCgNIC·9H_2O		EGCgINM·5H_2O		EGCgINA·3H_2O		EGCgINA	
	mean	SD	mean	SD	mean	SD	mean	SD	mean	SD
T_{max} (min)	7.50	2.74	20.00	10.95	30.00	0.00	30.00	24.49	160.00	61.97
C_{max} (ng/mL)	341.50	247.10	188.33	106.26	125.95	67.91	347.17	236.92	167.40	84.66
$AUC_{(0-t)}$ (min·ng/mL)	39796.33	26318.73	22064.75	3410.81	22636.28	9177.62	54560.42	21954.28	41937.08	12165.97
F_{rel}	1.00	NA	0.55	NA	0.57	NA	1.37	NA	1.05	NA
HL_Lambda_z (min)	249.35	60.73	341.71	212.97	263.74	68.31	352.61	79.85	350.83*	195.13

*Due to an insufficient number of data points in the elimination phase of the pharmacokinetic profile, C_{max} was included in the Lambda_z calculation during the noncompartmental analysis in WinNonlin.

EGCg, perhaps improving its bioavailability. When interpreting our data, it is important to note that we used a nonconventional gavage vehicle (corn oil) to prevent presolubilizing of the sieved crystalline forms. Our EGCg control peaked approximately 16.5 min more rapidly than previously published pharmacokinetic data at the same dose in rats using a saline gavage vehicle.[55] Furthermore, we previously assessed the pharmacokinetics of an EGCg nanolipidic particle suspension in 10% ethanol.[17] For an accurate comparison, we used a 10% ethanol vehicle for the control. This resulted in lower levels of free EGCg measured in the plasma (C_{max} = 116.57 ng/mL).[17] These variations illustrate the impact that gavage vehicle can have on pharmacokinetics. Nonetheless, the results presented in this paper should be considered a stand-alone comparison of EGCg and EGCg cocrystals in a common vehicle.

At first glance, it seems that cocrystallization might not be the most useful method for improving the bioavailability of EGCg, since only two cocrystals exhibited improved relative bioavailability and the increases were very modest (Table 3). Although we did not monitor the metabolic profile of the circulating EGCg, it is likely that the blunted bioavailability increases were due to the well-known metabolism issues with EGCg,[56] which is left unchecked in these cocrystal forms. An additional contributor to the observed relative bioavailability for this experiment is apparent when considering the variability for the EGCg control (Table 3). One of the experimental rats achieved three times higher plasma levels of free EGCg than observed in the other rats. This increased the variability and the C_{max} but did not change the T_{max}. We decided not to exclude this animal from the analysis. However, if this animal had been excluded as an outlier, the relative bioavailability for the cocrystal forms would have increased. Our pharmacokinetic study design utilized an n = 3. This decision was driven by our desire to minimize the use of animals and based on previous pharmacokinetic studies performed in our lab.[17,57] However, the pharmacokinetic study suffered from unexpected levels of variability, which should be considered when drawing conclusions from this data. The pharmacokinetic parameters presented in Table 3 include the means with standard deviations. For the EGCgINA, an asterisk marks the HL_Lambda_z, because there were insufficient data points in the elimination phase such that the C_{max} had to be included in the noncompartmental analysis in WinNonlin. This only occurred with the EGCgINA cocrystal because we did not expect such a robust change in the T_{max}.

Even though our new forms of EGCg did not lead to large increases in oral bioavailability, this does not mean that cocrystallization cannot benefit the commercialization of EGCg. The ability to have multiple solid forms of EGCg with different physicochemical properties and pharmacokinetic profiles could

be very useful. Further examination of Figure 10 indicates that some of the EGCg cocrystals exhibited different pharmacokinetic profiles. The EGCgINA·3H_2O and EGCgINA cocrystals not only had the highest relative bioavailabilities of the cocrystals that we evaluated but also resulted in higher concentrations of free EGCg after 60 and 120 min, respectively. This plateau effect could be useful for achieving more sustained levels of EGCg in the blood. Furthermore, because pharmaceutical and nutraceutical products often contain combinations of ingredients with synergistic effects, cocrystallization could be used to select forms with similar pharmacokinetics as the other ingredients. This would allow for optimization of the synergistic activities.

Our results generally support our hypothesis that reducing the solubility reduces the rate of dissolution and delays the time at which maximal plasma levels are reached (T_{max}). EGCgNIC·9H_2O was found to be the most water-soluble cocrystal form and had the most rapid T_{max} after free EGCg. EGCgINM·5H_2O and EGCgINA·3H_2O also had expected T_{max} values based upon the solubility experiments. However, EGCgINA peaked at 160 min (Table 3) and was found to exhibit similar solubility to that of EGCgINM·5H_2O and EGCgINA·3H_2O (Figure 9). This phenomenon cannot be explained by our solubility hypothesis. Normally, it might be reasonable to assume that other pharmacokinetic parameters are being changed, like elimination rate or metabolism. This would normally be attributed to some effect of the CCF. However, this cannot be the case for EGCgINA and EGCgINA·3H_2O since they have the same CCF. As expected, the hydrate exhibited slightly lower water solubility and peaked later in comparison to the other more soluble EGCg forms. Because anhydrous and hydrous forms were evaluated, we were able to conclude that the presence of INA does not explain the discrepancy observed with the EGCgINA cocrystal. Further studies are required to elucidate the cause of this anomaly. Nonetheless, it is very clear that cocrystallization can be used to generate novel forms of EGCg with modulated dissolution and pharmacokinetic profiles (see also Supporting Information).

In conclusion, the present study demonstrates how crystal engineering concepts can be utilized for isolating new cocrystals of EGCg and that with the aid of several crystallization techniques we were able isolate the first pure (i.e., nonsolvated, nonhydrated) crystal form of EGCg. However, cocrystallization might not be the best option for improving the bioavailability of BCS 3 compounds like EGCg, but it could be very useful when absorption kinetics is critical such as it is in synergistic and/or combination products. For example, selection of a cocrystal form that exhibits a dissolution rate-limited pharmacokinetic profile could achieve sustained plasma levels of free active ingredient similar to other sustained release preformulation techniques like transdermal delivery.[58] Sustained plasma levels are preferred so that the therapeutic bioactivity of the active ingredient is maintained for a longer duration. Even though transdermal delivery can also accomplish sustained plasma levels, it has numerous disadvantages to oral formulation such as complicated production, increased cost, and reduced patient compliance due to common side effects like skin irritation at the adhesion site.

This study therefore lends credence to the concept of using cocrystallization to modulate the pharmacokinetics of highly water-soluble compounds. In this study, we evaluated four new solid forms of EGCg with different solubility properties and consequent pharmacokinetic profiles. Although we confirmed that a single cocrystal with reduced solubility relative to a highly soluble pure form is unlikely to produce improved bioavailability, the ability to modulate the pharmacokinetic curve using crystal engineering could be very useful in the clinical translation of active ingredients. In theory, this could result in a superior bioactivity and therapeutic profile. Further studies are required to confirm this potential utility.

■ ASSOCIATED CONTENT

Ⓢ Supporting Information

IR, DSC, TGA, and PXRD patterns for the reported crystalline forms of EGCg. This material is available free of charge via the Internet at http://pubs.acs.org.

■ AUTHOR INFORMATION

Corresponding Author

*M.Z.: Phone: 813-974-3451; e-mail: xtal@usf.edu. D.S.: Phone: 813-974-9171; fax: 813-974-3078; e-mail: dshytle@health.usf.edu.

Present Address

⊥Department of Industrial and Physical Pharmacy, College of Pharmacy, Purdue University, West Lafayette, Indiana 47907, United States.

Notes

Authors are inventors on USF patent disclosures pertaining to these technologies.

■ ACKNOWLEDGMENTS

This work was supported by research grant number ARG2008 from the Johnnie B. Byrd, Sr. Alzheimer's Center & Research Institute (R.S. and M.Z.).

■ ABBREVIATIONS

EGCg, epigallocatechin 3-gallate; API, active pharmaceutical ingredient; INM, isonicotinamide; INA, isonicotinic acid; NIC, nicotinamide; NAC, nicotinic acid; EGCgNIC·9H_2O, EGCg:nicotinamide; EGCgINM·5H_2O, EGCg:isonicotinamide; EGCgINA·3H_2O, EGCg:isonicotinic acid; EGCgINA, EGCg:isonicotinic acid anhydrous; EGCgNAC·xH_2O, EGCg:nicotinic acid; PXRD, powder X-ray diffraction; DSC, differential scanning calorimeter; FT-IR, Fourier transform infrared spectroscopy; TGA, thermogravimetric analysis; AUC, area under curve

■ REFERENCES

(1) Hertog, M. G. Epidemiological evidence on potential health properties of flavonoids. *Proc. Nutr. Soc.* **1996**, *55* (1B), 385−97.

(2) Arts, I. C. A review of the epidemiological evidence on tea, flavonoids, and lung cancer. *J. Nutr.* **2008**, *138* (8), 1561S−1566S.

(3) Formica, J. V.; Regelson, W. Review of the biology of Quercetin and related bioflavonoids. *Food Chem. Toxicol.* **1995**, *33* (12), 1061−80.

(4) Hwang, J. T.; Ha, J.; Park, I. J.; Lee, S. K.; Baik, H. W.; Kim, Y. M.; Park, O. J. Apoptotic effect of EGCG in HT-29 colon cancer cells via AMPK signal pathway. *Cancer Lett.* **2007**, *247* (1), 115−21.

(5) Jung, Y. D.; Kim, M. S.; Shin, B. A.; Chay, K. O.; Ahn, B. W.; Liu, W.; Bucana, C. D.; Gallick, G. E.; Ellis, L. M. EGCG, a major component of green tea, inhibits tumour growth by inhibiting VEGF induction in human colon carcinoma cells. *Br. J. Cancer* **2001**, *84* (6), 844−50.

(6) Lim, Y. C.; Park, H. Y.; Hwang, H. S.; Kang, S. U.; Pyun, J. H.; Lee, M. H.; Choi, E. C.; Kim, C. H. (−)-Epigallocatechin-3-gallate (EGCG) inhibits HGF-induced invasion and metastasis in hypopharyngeal carcinoma cells. *Cancer Lett.* **2008**, *271* (1), 140−52.

(7) Wang, X.; Hao, M. W.; Dong, K.; Lin, F.; Ren, J. H.; Zhang, H. Z. Apoptosis induction effects of EGCG in laryngeal squamous cell carcinoma cells through telomerase repression. *Arch. Pharm. Res.* **2009**, *32* (9), 1263−9.
(8) Wang, Y. C.; Bachrach, U. The specific anti-cancer activity of green tea (−)-epigallocatechin-3-gallate (EGCG). *Amino Acids* **2002**, *22* (2), 131−43.
(9) Lin, C. L.; Chen, T. F.; Chiu, M. J.; Way, T. D.; Lin, J. K. Epigallocatechin gallate (EGCG) suppresses beta-amyloid-induced neurotoxicity through inhibiting c-Abl/FE65 nuclear translocation and GSK3 beta activation. *Neurobiol. Aging* **2009**, *30* (1), 81−92.
(10) Obregon, D. F.; Rezai-Zadeh, K.; Bai, Y.; Sun, N.; Hou, H.; Ehrhart, J.; Zeng, J.; Mori, T.; Arendash, G. W.; Shytle, D.; Town, T.; Tan, J. ADAM10 activation is required for green tea (−)-epigallocatechin-3-gallate-induced alpha-secretase cleavage of amyloid precursor protein. *J. Biol. Chem.* **2006**, *281* (24), 16419−27.
(11) Rezai-Zadeh, K.; Arendash, G. W.; Hou, H.; Fernandez, F.; Jensen, M.; Runfeldt, M.; Shytle, R. D.; Tan, J. Green tea epigallocatechin-3-gallate (EGCG) reduces beta-amyloid mediated cognitive impairment and modulates tau pathology in Alzheimer transgenic mice. *Brain Res.* **2008**, *1214*, 177−87.
(12) Rezai-Zadeh, K.; Shytle, D.; Sun, N.; Mori, T.; Hou, H.; Jeanniton, D.; Ehrhart, J.; Townsend, K.; Zeng, J.; Morgan, D.; Hardy, J.; Town, T.; Tan, J. Green tea epigallocatechin-3-gallate (EGCG) modulates amyloid precursor protein cleavage and reduces cerebral amyloidosis in Alzheimer transgenic mice. *J. Neurosci.* **2005**, *25* (38), 8807−14.
(13) Hwang, J. T.; Park, I. J.; Shin, J. I.; Lee, Y. K.; Lee, S. K.; Baik, H. W.; Ha, J.; Park, O. J. Genistein, EGCG, and capsaicin inhibit adipocyte differentiation process via activating AMP-activated protein kinase. *Biochem. Biophys. Res. Commun.* **2005**, *338* (2), 694−9.
(14) Wolfram, S. Effects of green tea and EGCG on cardiovascular and metabolic health. *J. Am. Coll. Nutr.* **2007**, *26* (4), 373S−388S.
(15) Cai, E. P.; Lin, J. K. Epigallocatechin Gallate (EGCG) and Rutin Suppress the Glucotoxicity through Activating IRS2 and AMPK Signaling in Rat Pancreatic beta Cells. *J. Agric. Food Chem.* **2009**, *57*, 9817−27.
(16) Lin, C. L.; Lin, J. K. Epigallocatechin gallate (EGCG) attenuates high glucose-induced insulin signaling blockade in human hepG2 hepatoma cells. *Mol. Nutr. Food Res.* **2008**, *52* (8), 930−9.
(17) Smith, A.; Giunta, B.; Bickford, P. C.; Fountain, M.; Tan, J.; Shytle, R. D. Nanolipidic particles improve the bioavailability and alpha-secretase inducing ability of epigallocatechin-3-gallate (EGCG) for the treatment of Alzheimer's disease. *Int. J. Pharmaceutics* **2010**, *389* (1−2), 207−12.
(18) Ando, S.; Kikuchi, J.; Fujimura, Y.; Ida, Y.; Higashi, K.; Moribe, K.; Yamamoto, K. Physicochemical characterization and structural evaluation of a specific 2:1 cocrystal of naproxen-nicotinamide. *J. Pharm. Sci.* **2012**, *101* (9), 3214−21.
(19) Cherukuvada, S.; Babu, N. J.; Nangia, A. Nitrofurantoin-p-aminobenzoic acid cocrystal: hydration stability and dissolution rate studies. *J. Pharm. Sci.* **2011**, *100* (8), 3233−44.
(20) Gao, Y.; Zu, H.; Zhang, J. Enhanced dissolution and stability of adefovir dipivoxil by cocrystal formation. *J. Pharm. Pharmacol.* **2011**, *63* (4), 483−90.
(21) Goud, N. R.; Gangavaram, S.; Suresh, K.; Pal, S.; Manjunatha, S. G.; Nambiar, S.; Nangia, A. Novel furosemide cocrystals and selection of high solubility drug forms. *J. Pharm. Sci.* **2012**, *101* (2), 664−80.
(22) Jung, M. S.; Kim, J. S.; Kim, M. S.; Alhalaweh, A.; Cho, W.; Hwang, S. J.; Velaga, S. P. Bioavailability of indomethacin-saccharin cocrystals. *J. Pharm. Pharmacol.* **2010**, *62* (11), 1560−8.
(23) McNamara, D. P.; Childs, S. L.; Giordano, J.; Iarriccio, A.; Cassidy, J.; Shet, M. S.; Mannion, R.; O'Donnell, E.; Park, A. Use of a glutaric acid cocrystal to improve oral bioavailability of a low solubility API. *Pharm. Res.* **2006**, *23* (8), 1888−97.
(24) Okaniwa, M.; Imada, T.; Ohashi, T.; Miyazaki, T.; Arita, T.; Yabuki, M.; Sumita, A.; Tsutsumi, S.; Higashikawa, K.; Takagi, T.; Kawamoto, T.; Inui, Y.; Yoshida, S.; Ishikawa, T. Design and synthesis of novel DFG-out RAF/vascular endothelial growth factor receptor 2 (VEGFR2) inhibitors: 2. Synthesis and characterization of a novel imide-type prodrug for improving oral absorption. *Bioorg. Med. Chem.* **2012**, *20* (15), 4680−92.
(25) Rahman, Z.; Samy, R.; Sayeed, V. A.; Khan, M. A. Physicochemical and mechanical properties of carbamazepine cocrystals with saccharin. *Pharm. Dev. Technol.* **2012**, *17* (4), 457−65.
(26) Schultheiss, N.; Newman, A. Pharmaceutical Cocrystals and Their Physicochemical Properties. *Cryst. Growth Des.* **2009**, *9* (6), 2950−2967.
(27) Smith, A. J.; Kavuru, P.; Wojtas, L.; Zaworotko, M. J.; Shytle, R. D. Cocrystals of quercetin with improved solubility and oral bioavailability. *Mol. Pharmaceutics* **2011**, *8* (5), 1867−76.
(28) Tsutsumi, S.; Iida, M.; Tada, N.; Kojima, T.; Ikeda, Y.; Moriwaki, T.; Higashi, K.; Moribe, K.; Yamamoto, K. Characterization and evaluation of miconazole salts and cocrystals for improved physicochemical properties. *Int. J. Pharmaceutics* **2011**, *421* (2), 230−6.
(29) Yadav, A. V.; Dabke, A. P.; Shete, A. S. Crystal engineering to improve physicochemical properties of mefloquine hydrochloride. *Drug Dev. Ind. Pharm.* **2010**, *36* (9), 1036−45.
(30) Shutava, T. G.; Balkundi, S. S.; Lvov, Y. M. (−)-Epigallocatechin gallate/gelatin layer-by-layer assembled films and microcapsules. *J. Colloid Interface Sci.* **2009**, *330* (2), 276−83.
(31) Ullmann, U.; Haller, J.; Decourt, J. D.; Girault, J.; Spitzer, V.; Weber, P. Plasma-kinetic characteristics of purified and isolated green tea catechin epigallocatechin gallate (EGCG) after 10 days repeated dosing in healthy volunteers. *Int. J. Vitam. Nutr. Res.* **2004**, *74* (4), 269−78.
(32) Swezey, R. R.; Aldridge, D. E.; LeValley, S. E.; Crowell, J. A.; Hara, Y.; Green, C. E. Absorption, tissue distribution and elimination of 4-[(3)h]-epigallocatechin gallate in beagle dogs. *Int. J. Toxicol.* **2003**, *22* (3), 187−93.
(33) Cai, Y.; Anavy, N. D.; Chow, H. H. Contribution of presystemic hepatic extraction to the low oral bioavailability of green tea catechins in rats. *Drug Metab. Dispos.* **2002**, *30* (11), 1246−9.
(34) Hu, B.; Ting, Y.; Yang, X.; Tang, W.; Zeng, X.; Huang, Q. Nanochemoprevention by encapsulation of (−)-epigallocatechin-3-gallate with bioactive peptides/chitosan nanoparticles for enhancement of its bioavailability. *Chem. Commun. (Cambridge)* **2012**, *48* (18), 2421−3.
(35) *Bruker APEX2* (Version 2008.1−0); Bruker AXS Inc.: Madison, WI, 2008.
(36) *SAINT Data Reduction Software*; Bruker AXS Inc.: Madison, WI, 2009.
(37) Sheldrick, G. M. *SADABS. Program for Empirical Absorption Correction*; University of Gottingen: Gottingen, Germany, 2008.
(38) Farrugia, L. J. WinGX suite for single crystal small molecule crystallography. *J. Appl. Cryst.* **1999**, *32*, 837−838.
(39) Sheldrick, G. M. *SHELXL-97. Program for the Refinement of Crystal Structures*; University of Gottingen: Gottingen, Germany, 1997.
(40) Sheldrick, G. M. Phase Annealing in SHELX-90: Direct Methods for Larger Structures. *Acta Crystallogr.* **1990**, *A46*, 467−473.
(41) Lambert, J. D.; Lee, M. J.; Diamond, L.; Ju, J.; Hong, J.; Bose, M.; Newmark, H. L.; Yang, C. S. Dose-dependent levels of epigallocatechin-3-gallate in human colon cancer cells and mouse plasma and tissues. *Drug Metab. Dispos.* **2006**, *34* (1), 8−11.
(42) Sparidans, R. W.; Lagas, J. S.; Schinkel, A. H.; Schellens, J. H.; Beijnen, J. H. Liquid chromatography-tandem mass spectrometric assays for salinomycin in mouse plasma, liver, brain and small intestinal contents and in OptiMEM cell culture medium. *J. Chromatogr., B: Analyt. Technol. Biomed. Life Sci.* **2007**, *855* (2), 200−10.
(43) Wang, M.; Miksa, I. R. Multi-component plasma quantitation of anti-hyperglycemic pharmaceutical compounds using liquid chromatography-tandem mass spectrometry. *J. Chromatogr., B: Analyt. Technol. Biomed. Life Sci.* **2007**, *856* (1−2), 318−27.
(44) Wang, Z.; Hop, C. E.; Leung, K. H.; Pang, J. Determination of in vitro permeability of drug candidates through a caco-2 cell monolayer by liquid chromatography/tandem mass spectrometry. *J. Mass Spectrom.* **2000**, *35* (1), 71−6.

(45) Dube, A.; Nicolazzo, J. A.; Larson, I. Chitosan nanoparticles enhance the intestinal absorption of the green tea catechins (+)-catechin and (−)-epigallocatechin gallate. *Eur. J. Pharm. Sci.* **2010**, *41* (2), 219−25.
(46) Kale, A.; Gawande, S.; Kotwal, S.; Netke, S.; Roomi, W.; Ivanov, V.; Niedzwiecki, A.; Rath, M. Studies on the effects of oral administration of nutrient mixture, quercetin and red onions on the bioavailability of epigallocatechin gallate from green tea extract. *Phytother. Res.* **2010**, *24* (Suppl 1), S48−55.
(47) Landis-Piwowar, K. R.; Huo, C.; Chen, D.; Milacic, V.; Shi, G.; Chan, T. H.; Dou, Q. P. A novel prodrug of the green tea polyphenol (−)-epigallocatechin-3-gallate as a potential anticancer agent. *Cancer Res.* **2007**, *67* (9), 4303−10.
(48) Sekiguchi, K.; Obi, N. Studies on Absorption of Eutectic Mixture. I. A Comparison of the Behavior of Eutectic Mixture of Sulfathiazole and that of Ordinary Sulfathiazole in Man. *Chem. Pharm. Bull* **1961**, *9*, 866−872.
(49) Hickey, M. B.; Peterson, M. L.; Scoppettuolo, L. A.; Morrisette, S. L.; Vetter, A.; Guzman, H.; Remenar, J. F.; Zhang, Z.; Tawa, M. D.; Haley, S.; Zaworotko, M. J.; Almarsson, O. Performance comparison of a co-crystal of carbamazepine with marketed product. *Eur. J. Pharm. Biopharm.* **2007**, *67* (1), 112−9.
(50) Bak, A.; Gore, A.; Yanez, E.; Stanton, M.; Tufekcic, S.; Syed, R.; Akrami, A.; Rose, M.; Surapaneni, S.; Bostick, T.; King, A.; Neervannan, S.; Ostovic, D.; Koparkar, A. The co-crystal approach to improve the exposure of a water-insoluble compound: AMG 517 sorbic acid co-crystal characterization and pharmacokinetics. *J. Pharm. Sci.* **2008**, *97* (9), 3942−56.
(51) Cheney, M.; Shan, N.; Healey, E.; Hanna, M.; Wojtas, L.; Zaworotko, M. J.; Sava, V.; Song, S.; Sanchez-Ramos, J. Effects of Crystal Form on Solubility and Pharmacokinetics: A Crystal Engineering Case Study of Lamotrigine. *Cryst. Growth Des.* **2010**, *10* (1), 394−405.
(52) Stanton, M. K.; Kelly, R. C.; Colletti, A.; Kiang, Y. H.; Langley, M.; Munson, E. J.; Peterson, M. L.; Roberts, J.; Wells, M. Improved pharmacokinetics of AMG 517 through co-crystallization. Part 1: comparison of two acids with corresponding amide co-crystals. *J. Pharm. Sci.* **2010**, *99* (9), 3769−78.
(53) Weyna, D. R.; Cheney, M. L.; Shan, N.; Hanna, M.; Zaworotko, M. J.; Sava, V.; Song, S.; Sanchez-Ramos, J. R. Improving Solubility and Pharmacokinetics of Meloxicam via Multiple-Component Crystal Formation. *Mol. Pharmaceutics* **2012**, *9* (7), 2094−2102.
(54) Cheney, M. L.; Weyna, D. R.; Shan, N.; Hanna, M.; Wojtas, L.; Zaworotko, M. J. Coformer selection in pharmaceutical cocrystal development: a case study of a meloxicam aspirin cocrystal that exhibits enhanced solubility and pharmacokinetics. *J. Pharm. Sci.* **2011**, *100* (6), 2172−81.
(55) Lin, L. C.; Wang, M. N.; Tseng, T. Y.; Sung, J. S.; Tsai, T. H. Pharmacokinetics of (−)-epigallocatechin-3-gallate in conscious and freely moving rats and its brain regional distribution. *J. Agric. Food Chem.* **2007**, *55* (4), 1517−24.
(56) Warden, B. A.; Smith, L. S.; Beecher, G. R.; Balentine, D. A.; Clevidence, B. A. Catechins are bioavailable in men and women drinking black tea throughout the day. *J. Nutr.* **2001**, *131* (6), 1731−7.
(57) Smith, A. J.; Kavuru, P.; Wojtas, L.; Zaworotko, M. J.; Shytle, R. D. Cocrystals of quercetin with improved solubility and oral bioavailability. *Mol. Pharmaceutics* **2011**, *8* (5), 1867−76.
(58) Zobrist, R. H.; Schmid, B.; Feick, A.; Quan, D.; Sanders, S. W. Pharmacokinetics of the R- and S-enantiomers of oxybutynin and N-desethyloxybutynin following oral and transdermal administration of the racemate in healthy volunteers. *Pharm. Res.* **2001**, *18* (7), 1029−34.